Astronomy & Astrophysics manuscript no. May 13, 2003
(DOI: will be inserted by hand later)

Direct spectroscopic analysis of SN1999aa

G. Garavini[1], G. Folatelli[1], A. Goobar[1],S. Nobili[1],P. Nugent............

Department of Physics, Stockholm University,

SCFAB, S–106 91 Stockholm, Sweden

Abstract. We present direct analysis of the peculiar Type Ia supernova SN 1999aa in NGC 2595. This supernova has been suggested as a possible link between peculiar 91T-like and *Branch normals*. Our data set includes 25 optical spectra between -11 and +58 days with respect to B-band light curve maximum. We compare the observations with synthetic SYNOW spectra. In the early epochs, evidence is found for carbon at high velocities. Thus, the derived atmosphere properties soon after the explosion are consistent with the expectations for a high temperature unburned C+O rich region.

The first clear sign of SiII λ6355 Å characteristic for Type Ia supernovae, is found at day -7 and its velocity remains constant over time. We note a similar behavior for SN 1991T, SN 1997br and SN 2000cx. The implications for supernova hydrodynamical models are discussed briefly.

1. Introduction

Because of the homogeneity of their brightness Type Ia supernovae (SNIa) have become an excellent tool for distance estimates. The intrinsic spread in their absolute B magnitude is less than 0.4 mag and it can be corrected through empirical correlations to 0.14 mag (Phillips et al., 1999), making high redshift Type Ia SNe a powerful tool for the determination of cosmological parameters (Goobar & Perlmutter, 1995; Perlmutter et al., 1999; Riess et al., 1998).

Cosmological implications derived from supernovae rely on the assumption that distant SNe explosions are mere copies of the better known nearby ones. The increasing number of high quality data-sets of low redshift supernovae is shedding new light on diversities found among these objects. Studying and understanding the (in)homogeneity within the Ia class of SNe is of vital importance to pursue precision cosmological measurements and to clarify issues like brightness evolution effects and classification of peculiar supernovae.

With this goal the SCP coordinated an extensive campaign for finding a large number of nearby Type Ia supernovae and to obtain extensive follow-up observations during the spring of 1999, (Aldering, 2000; Nugent & Aldering, 2000). The subject of this work, SN 1999aa, was followed in this campaign and has been discussed as a very interesting object by several authors (Branch, 2000; Branch et al., 2001; Li et al., 2001b). It has been proposed as a key object to connect the peculiar slow decliner Type Ia SNe (SN 1991T-like) to the 'Branch-normal', which may help in understanding the physical origin of the observed diversities. The paper is organized as follows. The spec-

Send offprint requests to: G. Garavini , gabri@physto.se

troscopy data of SN 1999aa and a short description of the data reduction scheme are presented in section 2. An introduction on supernovae theory and modeling is given in section 3. A detailed description of the spectra time sequence is given in section 4 where we present a detailed comparison of SN 1999aa spectra with public data of spectroscopically peculiar and normal supernovae. The analysis of the velocities inferred from several spectral features are shown and discussed in section 5. Synthetic spectra produced with the highly parametrized SYNOW code are explored in section 6 and our final considerations about supernovae models and physics are given in section 7 and 8.

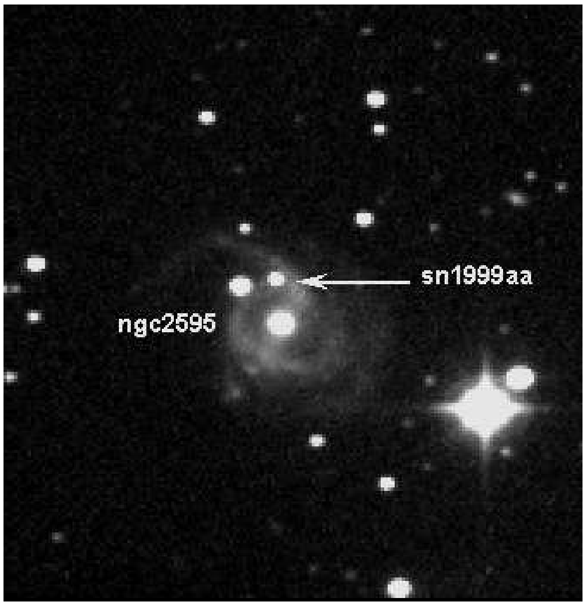

Fig. 1. SN 1999aa in its host galaxy NGC 2595. R.A. = $8^h27^m42^s.03$, Decl. = $+21^o29'14".8$ (equinox 2000.0).

2. Data and data reduction

Arbour (1999), Qiao et al. (1999) and Nakano et al. (1999) reported the discovery of SN 1999aa in the galaxy NGC 2595 measuring its position as R.A. = $8^h27^m42^s.03$, Decl. = $+21^o29'14".8$ (equinox 2000.0) on an unfiltered CCD image taken on Feb. 11.0166 UT. Filippenko et al. (1999) noted that it was a 91T-like peculiar Type Ia supernova based on a spectrum on February the 12th . Fig. 1 shows the position of SN 1999aa and its host galaxy. NGC 2595 is a SBc type with a compact blue core and blue spiral arms at redshift $z = 0.0146$ (The recession velocity of the host galaxy, determined from narrow H-alpha and [N II] emission, is 4485 km/s). Based on the Schlegel et al. (1998) model the reddening due to the milky way for SN 1999aa is $E(B-V) = 0.04$ mag. Krisciunas et al. (2000) estimated a negligible host galaxy reddening. The SCP campaign follow-up of this supernova consists in 25 different optical spectra ranging between 11 before and 58 days after maximum (in this work the epoch will be given with respect to the maximum B light) using 5 different instruments. Specifications of the data set are provided in Tab. 1 and the spectral time sequence is shown in Fig. 2.

All the raw data were analyzed with a common reduction scheme using standard IRAF routines. The two-dimensional images were bias-subtracted and flat-fielded using calibration images taken with the same instrument setting as the SN spectra and during the same night of observation. The sky background subtraction was performed on the resulting images using a fitted model of the sky and the sky spectrum itself was extracted for further checks on the wavelength calibration. The supernova spectrum was then extracted using the variance weighted optimal aperture extraction method (Horne, 1986). During the observations several arc lamp exposures were taken in order to calculate the dispersion solution and convert the pixel scale to wavelength for each given night. An atmospheric extinction correction was applied using a tabulated average extinction provided by the observatory. The accuracy of the calibration was checked against sky lines and generally found to be consistent within 2 Å. Spectrophotometric standard stars were observed during each night and were used to flux calibrate the SN spectra. A comparison between observations of different standard stars during the

JD -2400000	Epoch ref B_{max}	Telescope	Instrument	λ Region Å
51223.38	-11	NOT 2.6m	ALFOSC	3014-8972
51223.38	-11	NOT 2.6m	ALFOSC	3865-10032
51231.35	-3	NOT 2.6m	ALFOSC	2990-8857
51231.35	-3	NOT 2.6m	ALFOSC	3900-10025
51234.71	-1	Lick 3m	KAST	3279-5430
51234.71	-1	Lick 3m	KAST	5019-10474
51239.68	+5	MDM 2.4m	MARK III	3871-8806
51239.68	+6	MDM 2.4m	MARK III	3870-8808
51247.63	+14	APO 3.5m	DIS	3627-5887
51247.63	+14	APO 3.5m	DIS	4865-10333
51253.37	+19	NOT 2.6m	ALFOSC	2963-8862
51253.39	+19	NOT 2.6m	ALFOSC	3879-9994
51258.51	+25	CTIO 4m	RCSP	3210-9208
51261.54	+28	CTIO 4m	RCSP	3238-9237
51261.54	+28	CTIO 4m	RCSP	3238-9237
51266.53	+33	CTIO 4m	RCSP	3217-9199
51266.53	+33	CTIO 4m	RCSP	3217-9199
51273.62	+40	APO 3.5m	DIS	3616-5877
51273.62	+40	APO 3.5m	DIS	4860-10330
51282.67	+47	Lick 3m	KAST	3304-5462
51282.67	+47	Lick 3m	KAST	5003-10429
51286.63	+51	APO 3.5m	DIS	3615-5874
51286.63	+51	APO 3.5m	DIS	4863-10325
51293.71	+58	Lick 3m	KAST	3251-5390
51293.71	+58	Lick 3m	KAST	5214-7962

Table 1. Data set specification.

same night is used to check for possible systematic errors. In most of the cases the total exposure time was divided in different exposures in order to allow the elimination of the effect of cosmic rays on the final spectrum. A correction for Milky-Way extinction was applied using the standard procedure in (Cardelli et al., 1989) and assuming $R_V = 3.1$. Finally, the host galaxy spectrum was subtracted. No corrections for the telluric lines or for residual fringing patterns were performed because they do not affect our analysis. For a complete description of the data reduction methodology see (Folatelli et al., 2003a).

3. Models for Type Ia SNe

The most widely accepted model for Type Ia supernovae incorporates a degenerate C+O white dwarf (WD) accreting material through an overflow from a companion star (Wheeler et al., 1990; Filippenko, 1997). As the mass of the WD exceeds the Chandrasekhar limit the object

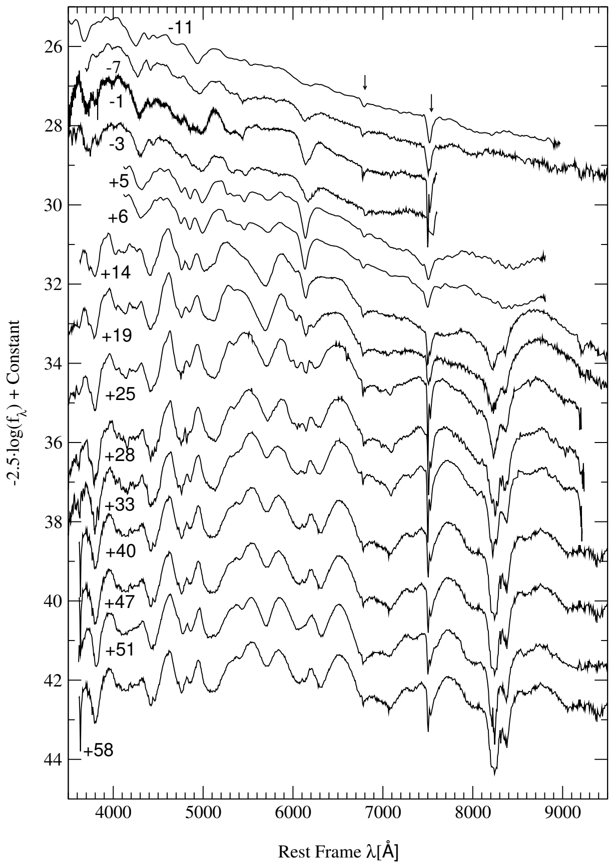

Fig. 2. SN 1999aa spectral time sequence. The epochs are referred to B-band maximum light. The two arrows mark the uncorrected atmospheric absorptions

starts contracting resulting in a compression of the star core and to an increasing of the central temperature that triggers thermonuclear reactions. The energy so released increases the temperature and consequently accelerates the thermonuclear reactions. Convective and conductive neutrino cooling work in slowing down the nuclear process, the net effect however eventually results in a rise of the central temperature leading to the expansion of the burning material (thermonuclear runaway (Hoyle, 1960; Hillebrandt et al., 2000)). The density at which the ignition starts is thought to depend on the accretion history of the WD. Fast accretion produces higher central temperatures and lower ignition densities. Most of the energy released during the explosion is due to the explosive burning of carbon and oxygen, thus the energy produced depends strongly on the initial composition of the WD. A major part of the energy production occurs in a thin flame propagating outwards. Carbon and oxygen burning proceeds then toward the external layers subsonically (*deflagration*) (Nomoto et al., 1984). The innermost layers are then burned completely to statistical equilibrium composition (NSE) forming the iron-peak core of the supernova. The energy produced during the thermonuclear burning fuels the expansion but not the luminosity that it powered up by the radioactive decay ^{56}Ni$\rightarrow^{56}$Co$\rightarrow^{56}$Fe. To match the observed intermediate mass elements (IME) composition,Branch et al. (1993), the models require the burning front to accelerate and reach the external layer. The local densities and temperature of the external layers are too low for the nuclear burning to reach statistical equilibrium. Incomplete Si-burning and unburnt C+O compositions are then excpected to be present in the outermost layers. In the delayed detonation hydrodynamical models the deflagration phase is followed by a supersonic burning period, (*detonation*) (Khokhlov, 1991; Yamaoka et al., 1992; Woosley et al., 1986). The deflagration to detonation transition (DDT) is usually parameterized by the transition density ρ_{tr}. The lower ρ_{tr} the less ^{56}Ni is produced and the intermediate mass elements are produced at lower external radii because of a shorter pre-expansion phase. The same effect is produced by a lower C/O ratio, (Höflich et al., 1998). Because of the lower energy production, the transition density is reached later in time, allowing for a longer expansion and then narrower region dominated by IME. One-dimensional delayed-detonation models have been successful in reproducing many observed characteristic of Type Ia supernovae but a complete description of the propagation of turbulent thermonuclear flame needs three-dimensional simulations. As pointed out by Gamezo et al. (2003) in a highly convoluted turbulent flame scenario the convective flows continuously take external material to the interior of the star keeping an active burning in the inner layers of the expanding atmosphere. While the expansion proceeds the density decreases. Intermediate mass elements are formed for densities lower than $5 \cdot 10^7$ gr/cm^3 and the burning stops completly for densities lower than 10^6 gr/cm^3 The unburnt carbon and oxygen should then produce visible spectral features at different radii down to the center of the star. For an extensive review of the theoretical models and observations see (Hillebrandt et al., 2000; Leibundgut et al., 2000; Branch et al., 2001; Filippenko, 1997). From an observational point of view the conclusion that SNe Ia are the result of the explosion of carbon-oxygen white dwarfs is supported mainly on the absence of H lines and their occurrence in Elliptical Galaxies. Prior light curve maximum normal type Ia SNe have spectra dominated by intermediate mass element such as SiII, SII, MgII, CaII and OI (Branch et al., 1993) and during the spectral evolution the absorptions due to this elements become weak and gradually more contaminated by iron-peak lines. The substitution is usually complete around 30 days after maximum when the supernova photosphere starts receding into the iron-peak core.

4. Spectra comparison

Objects such as SN 1991T, SN 1997br and SN 2000cx, represent a deviation from the impressive homogeneity of the spectral and photometric characteristics of SN explosions (Fisher et al., 1999; Li et al., 1999, 2001a) and therefore have raised the question whether they could be explained as a different physical phenomenon or rather they must be considered as extreme cases of the same process. When SN 1999aa was discovered and the first spectra circulated in the supernova community, the idea that this object could be helpful in addressing this question and that it could be used as a new supernovae prototype was proposed by several authors (Branch , 2001; Li et al., 2001b). This work should be viewed in that context.

4.1. Day 11 before maximum

The spectra of SN 1999aa and SN 1991T are very different from the normal SNe 1990N and 1994D around 11 days prior to the B-band light curve maximum, as shown in Fig. 3. The identification of the lines labeled here and in the following graphs are taken from Li et al. (1999, 2001a); Fisher et al. (1999); Patat et al. (1996); Mazzali et al. (1995); Kirshner et al. (1993); Jeffrey et al. (1992). Instead of the typical SiII, SII and MgII lines early spectra of these peculiar SNe are dominated by two deep absorption due to FeIII $\lambda\lambda 4404, 5129$ Å . SiIII $\lambda 4560$ Å is responsible for the smooth absorption on the red side of the first FeIII line ($\lambda 4404$ Å) and possibly smaller NiIII lines contribute near $\lambda\lambda$4700,5300, (Jeffrey et al., 1992; Ruiz-Lapuente et al., 1992). What mainly distinguish SN 1999aa from SN 1991T is the presence of the deep trough around 3800 Å, most probably CaII H&K but weaker compared to normals. The weak and broad line around 6150 Å could be due to SiII λ6355Å with a contamination from CII λ6580 Å as proposed by Fisher et al. (1999).

4.2. Day 3 before maximum

The first epoch SiII λ6355Å is clearly visible in our spectrum of SN 1999aa is day 7 before maximum, (Fig.2). By day -3, shown in Fig. 4, the spectrum goes through a big metamorphosis resembling more closely normal SNIa. The intermediate mass elements start dominating the spectrum while in SN 1991T CaII H&K and weak SiII lines, (in the 4000 Å and 6150 Å region respectively), are the only clear signs of them. FeIII and SiIII, $\lambda\lambda 4404, 4560$ Å are still intense and similar to those in SN 1991T. The redder of the two Fe III is getting broader like in SN 1994D for FeII contaminations. SII appears at this epoch show-

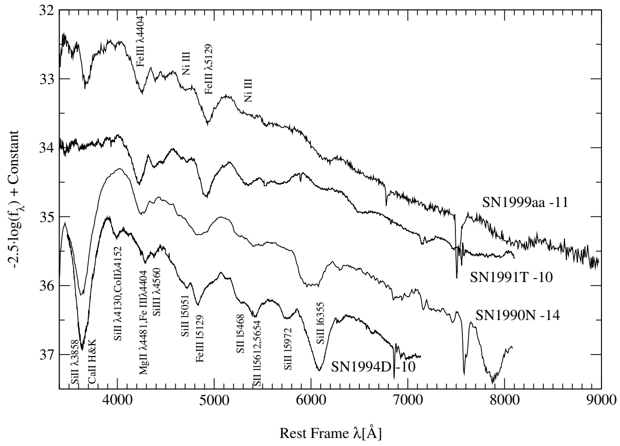

Fig. 3. The day -11 spectrum of SN 1999aa together with of SN 1991T, SN 1990N and SN 1994D from Mazzali et al. (1995); Mazzali (2001); Patat et al. (1996). Line identification is explained in the text.

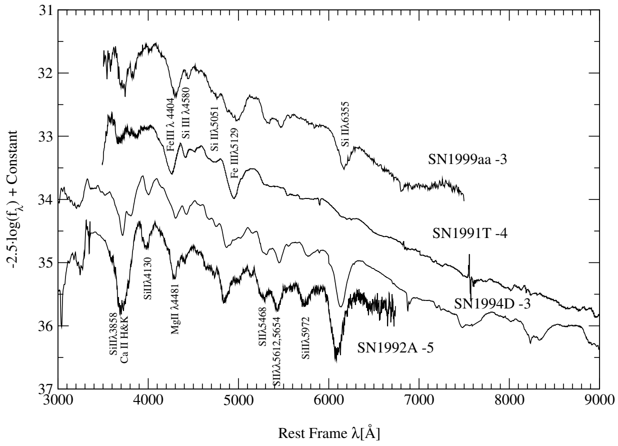

Fig. 4. The -3 spectrum of SN 1999aa together with of SN 1991T, SN 1992A and SN 1994D from Mazzali et al. (1995); Kirshner et al. (1993); Patat et al. (1996).

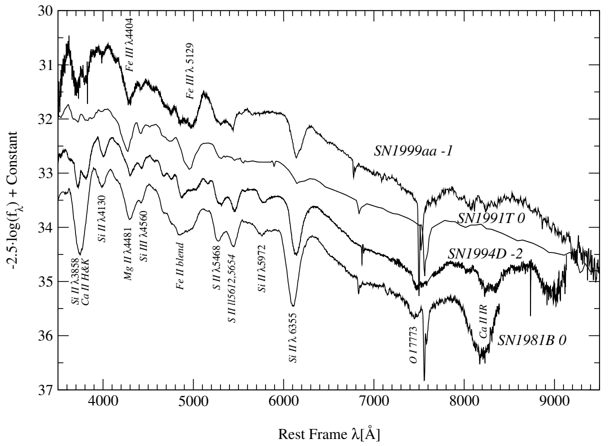

Fig. 5. The -1 day spectrum of SN 1999aa together with of SN 1991T, SN 1981B and SN 1994D from Phillips et al. (1992); Branch et al. (1983); Patat et al. (1996).

ing the typical 'W' shaped feature at $\lambda\lambda 5454, 5606$ Å that 91T-like SNe do not show. Silicon at $\lambda 6355$ Å is visible but fainter and redder than in normals. SiII $\lambda 5958$ Å is still not evident. If the evolution from CII to SiII proposed by Fisher et al. (1999) can be confirmed, SN 1991T at this epoch shows a weaker absorption than SN 1999aa, suggesting that the amount of SiII present in SN 1999aa is between that of normals and the truly peculiar 91T-like as well as for Ca. SN 1999aa already at this epoch appears generally much closer to normals compare to SN 1991T or SN 1997br, (see Fig.12 in Li et al., 1999).

4.3. Day 1 before maximum

The spectrum around maximum shown in Fig. 5 resembles the one of normal SNIa while SN 1991T is still dominated by FeIII lines with very weak SiII and Ca H&K lines. The CaII H&K region shows a characteristic split with the contamination from SiII $\lambda 3858$ Å as proposed by Nugent et al. (1997) and Lentz et al. (2000), where the red component is gaining strength. No sign of SiII $\lambda 5972$ Å is present, confirming again the overall weakness of the IME in this object. The CaII IR triplet $\sim \lambda 8000$ Å has two weak wiggles not present in SN 1981B but visible in SN 1994D. All the other major features are the same seen in normals.

4.4. Day 6 after maximum

The spectrum of one week after maximum, Fig. 6, is completely normal, showing now also the blue component of the SiII duo in the 5700-6200 Å region while SN 1991T (here at +9d) shows only weak SiII and SII lines. From Fig. 6 and from the spectra of other 91T-like supernovae shown in (Li et al., 1999) and (Li et al., 2001a) it is clear

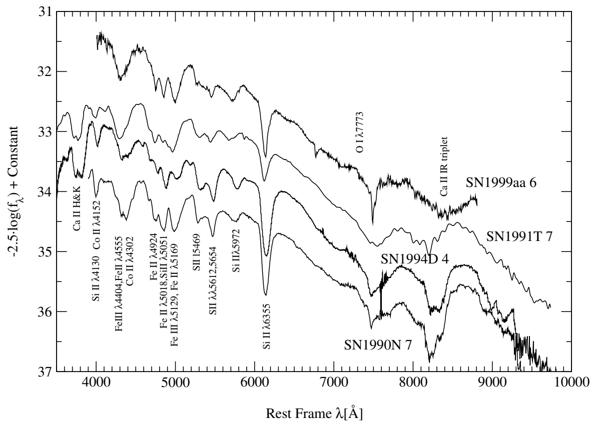

Fig. 6. The +6 day spectrum of SN 1999aa spectrum together with of SN 1991T, SN 1990N and SN 1994D from Mazzali et al. (1995); Jeffrey et al. (1992); Patat et al. (1996).

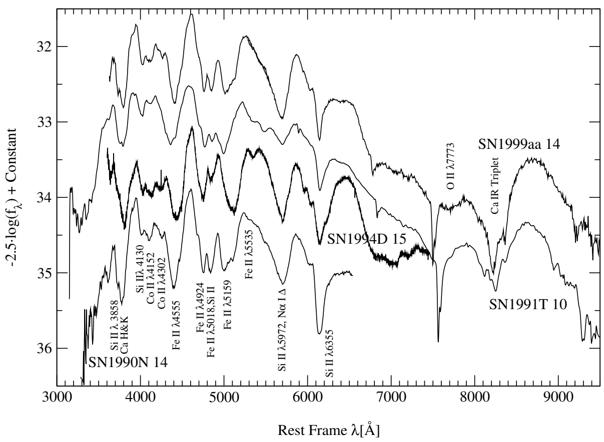

Fig. 7. The +14 day spectrum of SN 1999aa spectrum together with of SN 1991T, SN 1990N and SN 1994D from Mazzali et al. (1995); Leibundgut et al. (1991); Patat et al. (1996).

that the general trend for this objects is to have still at this epoch very weak intermediate mass elements components and a persistent dominant presence of highly ionized Fe, while in the normal SNe iron-peak elements as CoII and FeII start to appear and CaII IR triplet and OI λ7773 Å are getting stronger. SN 1999aa is very similar to normal SNIa spectra at this epoch while, as reported in (Li et al., 1999) and (Li et al., 2001a) SN 1997br and SN 2000cx have an already massive contribution from low ionization iron-peak elements with SN 1997br more advanced in this transition compared to SN 1991T. This suggests a very interesting sequence among these objects in which the duration in the phase of the intermediate-mass elements is the shortest in SN 1997br and the longest for SN 1999aa with SN 1991T placed somewhere in the middle. For Branch normal supernovae this phase extends from well before maximum to a couple of weeks after. In the case of these peculiar objects instead it seems to vary in duration and phase in the time evolution. This is probably due to the ratio Fe-peak/IME abundances, their radial distribution and temperature profile.

4.5. Day 14 after maximum

In the next set of spectra at day 14 , shown in Fig. 7, SN 1991T is still completing its intermediate mass elements phase with distinct P-Cygni profile for SiII λ6355 Å with virtually no contaminations from FeII. The 'W' of SII has not yet blended with NaI as in the other objects. The overall contribution of SII, SiII and CaII to its evolution is consistently weaker then in typical Type Ia. In SN 1997br the bottom of SiII is flatted down by FeII lines (see Fig. 14 in Li et al., 1999). SN 1999aa is now completely indistinguishable from a normal supernova as SN 1990N with maybe the only exception of a slightly weaker SiII λ6355 Å. Small differences are visible anyway also among normals. SN 1994D has a small absorption around 5500 Å that the other three objects do not show and that is maybe visible in SN 1997br and identifiable as FeII λ5535 Å.

4.6. Day 25 after maximum

As in the previous figure, the main differences at +25 days, Fig. 8, are around 6000 Å probably due to different Si abundance among the different objects. SN 1991T here shows the FeII $\lambda\lambda$6238, 6246, 6456, 6516 Å structures and

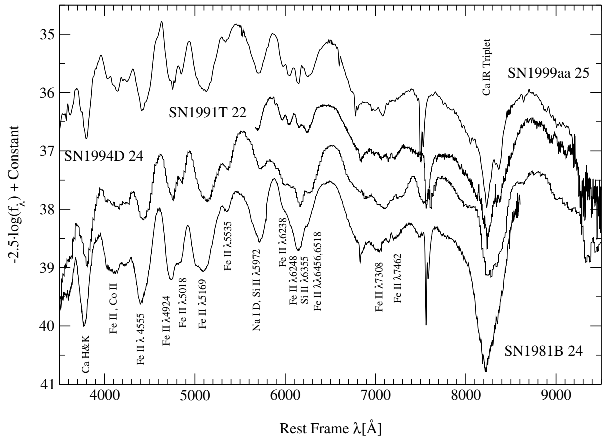

Fig. 8. The +25 day spectrum of SN 1999aa spectrum together with of SN 1991T, SN 1981B and SN 1994D from Mazzali et al. (1995); Branch et al. (1983); Patat et al. (1996).

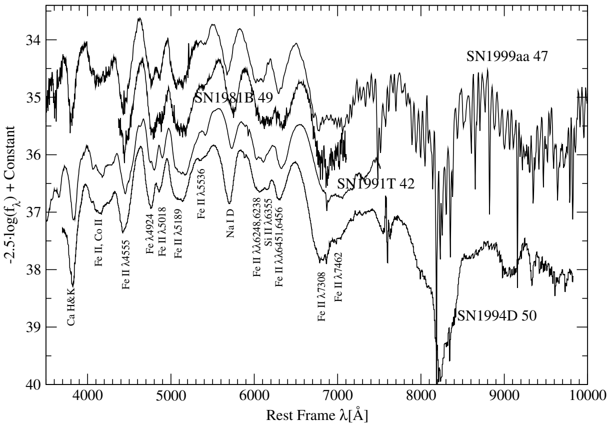

Fig. 9. The +47 day spectrum of SN 1999aa spectrum together with of SN 1991T, SN 1981B and SN 1994D from Gómez et al. (1998); Branch et al. (1983); Patat et al. (1996). The spectrum of SN 1999aa is affected by fringing which has not been corrected for.

just a very week SiII in the center while in SN 1999aa the SiII is a bit more evident and it gets even stronger in SN 1994D and SN 1981B. The trough near 5700Å due to SiII λ5972 Å and NaI D is strong in all the SNe. At the very red end of the spectra the four objects show the typical Ca II IR triplet as a very deep and broad absorption, SN 1999aa and SN 1991T show a second minimum in the red part of this features. At this stage the spectra are all dominated by FeII and CoII lines showing that they are formed mainly in the deep layers of the atmosphere.

4.7. Day 47 after maximum

Now, in the nebular phase, Fig. 9 shows that differences are still visible at +47 days. SN 1999aa is more similar to SN 1994D than to SN 1991T. In the λ4200 Å region of the latter, two minima are visible and the red edge is flat. The absorption at λ4924Å is deeper in SN 1994D then in SN 1999aa which has a stronger Fe λ5536 Å line. SN 1994d has still a hint of Si II λ6355 Å not present in SN 1999aa and SN 1991T but probably visible in the spectrum of SN 1981B. At the red end of the spectra of SN 19994D and SN 1999aa strong CA II IR triplet are visible. The spectrum of SN 1999aa suffers from some fringing that has not been corrected in the reduction phase since it does not affect the results of our analysis. Other small differences can be identified in the four spectra even at this epoch confirming that the overall evolution of the SN spectra has to be considered if we want really to understand the physics behind the peculiarities of the different objects.

5. Expansion Velocities

The expansion velocities as computed from fits to the minima of the lines can give help in investigating the physics of the supernova explosion.

The weighted fit of the minima was done using a non-linear Marquard-Levemberg minimization procedure (Marquardt, 1963) applied on a Gaussian profile model. The minimum of the line was considered to be the center of the Gaussian and the fit uncertainty its statistical error. This is usually of the order of few km/s since the high signal to noise ratio of our data and thus is not shown on the graphs. For a quantitative study however the systematic uncertainties on the profile model chosen and on the wavelength range selected should be considered. The analysis presented in this work is not quantitative and thus the systematic uncertainties are not taken into account. The general trend for the fitting was to consider the entire absorption of the P-Cygni profile when this was not distorted too much by contaminations in which case a line sample closer to the bottom was taken into account for the fit. In Figures 10-13 we show the velocities for CaII H&K, SiII (λ6355Å) and FeIII($\lambda\lambda$4404, 5129 Å) lines for SN 1999aa and other several public supernovae.

The CaII H&K velocities, Fig. 10, are in the normal range suggesting that if there is contamination from other elements (e.g SiIII, SiII, CoII) it is not much stronger then in other supernovae such as SN 1994D even if there is probably a trend to be a bit higher compare to the avarage of normal SNIa.

The SiII velocities, Fig. 11, are very interesting. If the absorption near 6150 Å was due only to SiII λ6355Å the velocities would have been monotonically decreasing with time as is clear for the normal SN 1994D, SN 1992A or for the sub-luminous SN 1999by and SN 1991bg. For SN 1999aa the first point, 11 days before maximum light, has the lowest velocity, this is consistent with CII being the major responsible for this line at this epoch. The late time behavior is also interesting, the line minimum remain practically stable during the first 20 days after maximum. This is usually interpreted as if the element layer in the supernova atmosphere was confined in a region above the photosphere, in this case around $10000 km/s$. The same trend is shown by SN 2000cx and SN 1991T with a velocity close to $12000 km/s$ and $9300 km/s$ respectively.

The velocities measured for the two big FeIII features, Fig. 12 and 13 , dominant in the pre-maximum spectra of the peculiar 91T-like SNe and disappearing within the first week after maximum light, are also interesting. In both cases SN 1999aa has the lowest velocities among SN 1991T, SN 1997br and SN 2000cx but the same slope. Fe III λ4404Å, Fig. 12, velocities are smaller by 2500 km/s with respect to SN 1991T and 3500 km/s with respect to SN 2000cx. Fe III λ5129Å, Fig. 13, velocities are instead still smaller but much closer to the ones of the other peculiar supernovae. This could be due to a higher contamination from SiII λ5051Å or FeII λ5018Å .

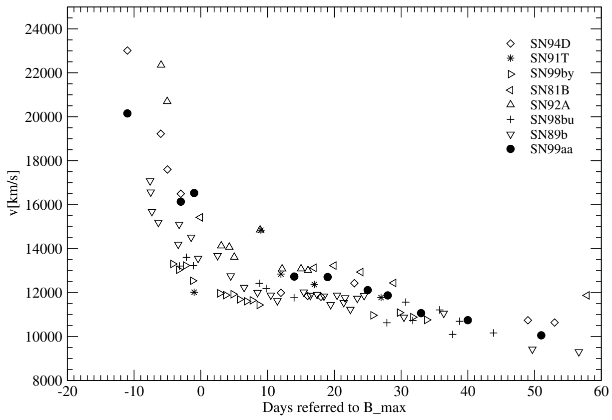

Fig. 10. Doppler shift of the Ca H&K line

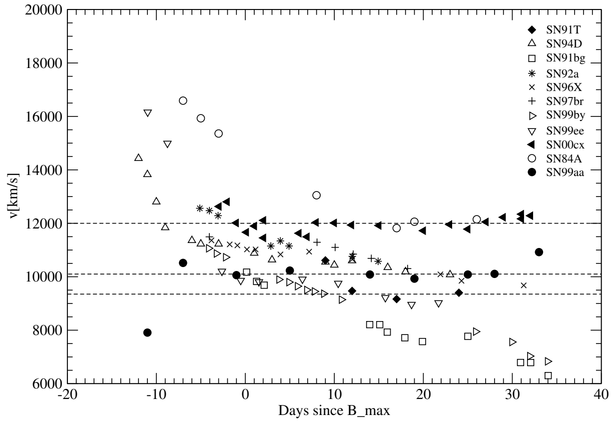

Fig. 11. Doppler shift of the SiII λ6350 Å line. Dashed lines indicating 12000 km/s, 10100km/s and 9350km/s.

Generally the velocities ranges of SN 1999aa line are quite consistent with a normal supernovae. The major peculiarity is the restricted atmosphere region in which SiII is present that makes clearly appear this ion only one week before maximum light.

6. Synthetic Spectra

In the previous sections we have taken an extensive look at the spectral features characteristics and evolution and enumerated the more evident differences in appearing

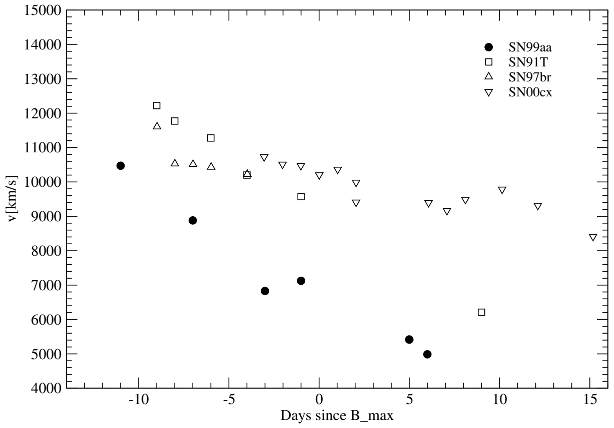

Fig. 12. Doppler shift of the FeIII λ4404 Å line

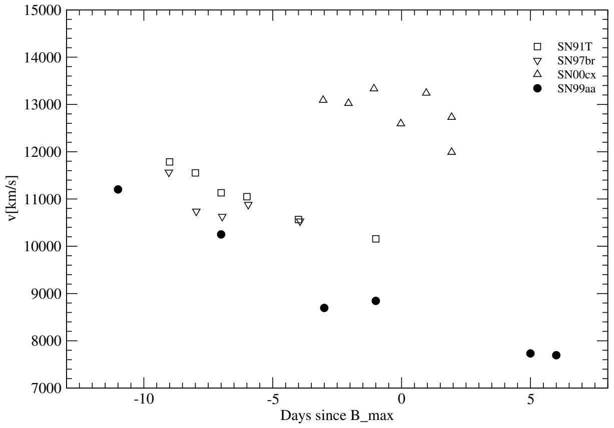

Fig. 13. Doppler shift of the FeIII λ5129 Å line

among normal, peculiar supernovae and SN 1999aa. Here we turn to a more quantitative analysis. We used SYNOW, (Fisher et al., 1997, 1999), to produce synthetic spectra and to investigate line identification and velocities ranges. SYNOW is a highly parametrized supernova synthetic spectrum code that assumes a sharp photosphere in spherical symmetry and treats the line formation in the expanding supernova atmosphere in Sobolev approximation using LTE occupation numbers and a resonance scattering source function. The synthetic spectrum is computed considering the different selected ions and values of the input parameters. The parameters for each ion are: the velocity v_{phot} at which the photosphere is placed and below which the atmosphere is considered optically thick. The temperature, T_{bb}, for the black body continuum, the optical depth for the ion reference line τ and its velocity range v_{min} and v_{max}. For each ion the excitation temperature, T_{exc}, is input. The radial distribution of the optical depth as a function of velocity is considered exponential with e-folding velocity v_e. In the present modeling scenario with the development of three dimensional asymmetric complete NLTE models, SYNOW can still give fast and useful information about the differences in the spectral composition and hints for the more rigorous hydrodynamical models. We have produced five synthetic spectra of SN 1999aa for epoch 11, and 1 before maximum light and 5, 14, 40 after.

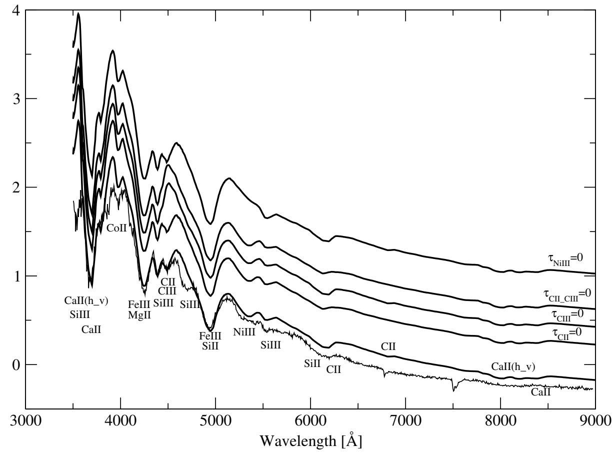

Fig. 14. Synthetic spectra compared with SN 1999aa spectrum for day -11. Solid lines from top to bottom:$\tau_{NiIII} = 0$. $\tau_{CIII,CII} = 0$,$\tau_{CIII} = 0$,$\tau_{CII} = 0$ and best match

6.1. -11 Days

In Fig. 14 we show the results for the best match synthetic spectrum computed using the parameters in table 2 togheter with the results exluding the NiIII, CII and CIII components.

The continuum black body temperature is 13700 K and the photosphere is placed at 11000 km/s. The dominant and characteristics features at this epoch are the two big FeIII lines, the first of which ($\sim$ λ4250 Å) has a small contribution of MgII. The small absorption around 4000

Å is identified as CoII. Note that in order to have the red edge and the minimum matching the data this ion needs to be detached from the photosphere. SiIII is responsible for the feature at 4400 Å and 5500 Å as well as for the one at 4700 Å as already identified by Jeffrey et al. (1992).

The only way we found to account for the complete structure of the CaII H&K features and for its velocity distribution (blue edge at 40000 km/s) is to introduce a high velocity component in addition to the one at v_{max}=19000km/s. At this epoch this allows us to 'fill-up' the whole spectral profile and at later epochs it will produce the observed blue wiggles of the CaII IR triplet as noticed already in Hatano et al. (1999b) for SN 1994D and analyzed by Kasen et al. (2003) for SN 2001el.

The features at 6150Å has a very broad profile, to reproduce it the usual SiII plus CII at high velocities have been used. As shown in Fig. 14 in absence of the C component and using only SiII the feature would look too blue and with the usual P-Cygni profile. In spite of trying many other possibilities, no other ion has shown a convincing contribution at this wavelengths. CII shows also a second a third smaller line at around λ6800Åand λ4500Å respectively close to the first telluric line and on the emission of SiIII at 4400 Å. In the spectral time sequence, Fig. 2, we can see that shape of this line changes at day -7 with the appearance of the first strong SiII λ6355 Å line at the right velocity, (Fig. 11). In our spectrum of SN 1999aa we find that the line on the red of SiIII λ4568 Å can be well matched by CIII λ4648.8ÅIts importance for a good match of the observed spectrum is shown in Fig. 14 where a series synthetic spectra with and without CIII components are compared.

The broad absorption at 5300 Å can be matched with NiIII with the same parameters as for FeIII. NiIII forms a line at λ 4613Å in our synthetic spectrum this is not visible due to the emission of CIII laying on the same region. The same region would show a better match by increasing the excitation temperature of SiIII but for consistency with the other ions parameters we decided to keep it fixed to 15000 K.

Ion	τ	v_{min} 10^3kms^{-1}	v_{max} 10^3kms^{-1}	T_{exc} 10^3K	v_e 10^3kms^{-1}
CaII	0.8	-	19	15	5.5
CaII	1	19	30	15	10
SiII	0.1	-	30	15	5
SiIII	0.6	12.5	15	15	3
MgII	0.1	-	30	15	5
CoII	0.3	15	17	10	3
FeIII	0.6	-	30	10	4
NiIII	1	-	30	5	15
CII	0.015	19	30	15	5
CIII	0.4	-	14.5	15	4

Table 2. Synow parameters for day -11. Vphot=11000km/s, $T_{bb} = 13700$

Small improvement in the the synthetic spectrum could be achieved introducing SiIV and OIII. The first would reduce the emission on the red edge of Ca H&K making the CoII line at 4000 Å have the right flux. The second would make slightly deeper the absorption of the first FeIII line. These ions, though, make their contribution only in regions were the absorption are blended with other lines, and thus their identification can not be proven or used in drawing any conclusion in our analysis.

6.2. -1 Days

By day -1, the spectrum as shown in Fig. 15 looks much more similar to normal SNeIa. SiII and SiIII have been introduced with a low maximum velocity in order to match the observed wavelength of the minima, see table 3 for details. SII, CoII and FeII line are well reproduced by detached layers while FeIII line needs $v_{max} = 12500$km/s.

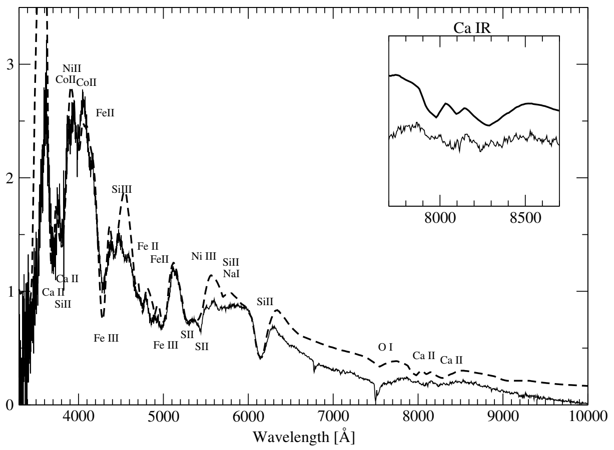

Fig. 15. Synthetic spectrum compared with SN 1999aa spectrum for day -1. The inset graph shows the velocity range match in the CaII IR triplet region.

The double component of CaII is needed at this epoch both in the H&K and IR triplet regions. The the blue minimum of the H&K components is reproduced by the high velocity component with v_{min} = 21000 km/s, the same matches the two small wiggles in the blue part of the CaII IR triplet as shown in the inset graph of Fig.15. The black body continuum does not match the observed spectrum above 6300 Å but nevertheless the wavelenght minima of the high velocity component of CaII IR triplet are well constrained.

NiII and NiIII are here introduced to improved the line profile reproduction of some line. NiII absorb the emission of the low velocity component of Ca H&K. NiIII falls in the middle of the 'W' shaped SII and flats down the emission in between the to lines. As for OIII and SiIV in the previous section the identification of this ions can not be claimed definitely but the improvement on the matching is somehow convincing.

Ion	τ	v_{min}	v_{max}	T_{exc}	v_e
		10^3kms^{-1}	10^3kms^{-1}	10^3 K	10^3kms^{-1}
CaII	3	-	18	5	6
CaII	2.5	21	25	5	5
OI	0.2	-	30	5	3
SiII	1	-	15	10	4
SiIII	0.4	-	14	10	5
SII	0.6	10	30	10	4
FeII	0.5	17	30	8	5
CoII	0.2	15	20	10	3
NaI	0.3	10	30	8	4
FeIII	0.5	-	12.5	6	3
NiIII	15	-	30	13	3
NiII	0.05	-	30	5	3

Table 3. Synow parameters for day -1. Vphot=9500km/s, $T_{bb} = 13500$

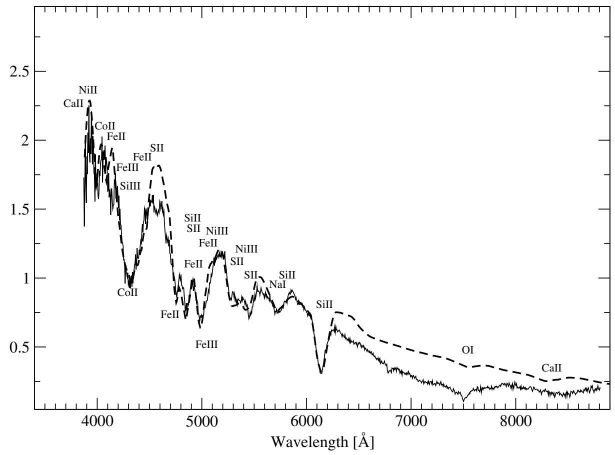

Fig. 16. Synthetic spectrum compared with SN 1999aa spectrum for day +5

6.3. +5 Days

In the synthetic spectrum for day 5 after maximum, shown in Fig. 16, highly ionized Ni, Si and Fe have lower optical depth than in the previous epoch analyzed, see table 4. The main contribution of NiIII is again in lowering the emission between the two SII features at 5400 Åbut in order to do so a very high excitation temperature is needed. FeIII and SiIII are blended in forming the big trough at 4400 Å together with CoII.

In order to reproduce the three distinct minima below 5000 Å , the FeII layer has to be detached and shallow in

Ion	τ	v_{min}	v_{max}	T_{exc}	v_e
		$10^3 \mathrm{km} s^{-1}$	$10^3 \mathrm{km} s^{-1}$	10^3K	$10^3 \mathrm{km} s^{-1}$
CaII	20	-	30	5	3
OI	0.1	-	30	5	3
SiII	1.5	10	15	8	3
SiIII	0.3	16	30	5	3
SII	0.4	10	15	5	3
FeII	1.5	11	15	5	3
CoII	0.8	13	30	5	3
NaI	0.4	-	20	5	5
FeIII	0.09	-	30	5	3
NiIII	8	-	30	13	3
NiII	0.1	-	30	10	3

Table 4. Synow parameters for day +5. Vphot=9000km/s, $T_{bb} = 12000$

velocity space, otherwise the lines tend to blend together forming a single broad feature as seen in SN 1981G.

SiII λ6150 Å is reproduced by a thin layer in the same velocity range as FeII. The feature at 5700 Å is probably identifiable manly with NaI, the SiII component results to be weak thanks to the low excitation temperature at which has been introduced; a higher temperature would create a redder features than the one seen in our data.

Unfortunately our spectra does not cover the region below 3900 Å and the Ca IR triplet is too weak to fully determine whether there is still need for a high velocity component.

6.4. +14 Days

In the synthetic spectrum at day +14, shown in Fig. 17, most of the lines can be identified as FeII, see table 5. As at the previous epoch, in order to reproduce the three different minima in the FeII blend region we use a minimum velocity higher than that of the photosphere.

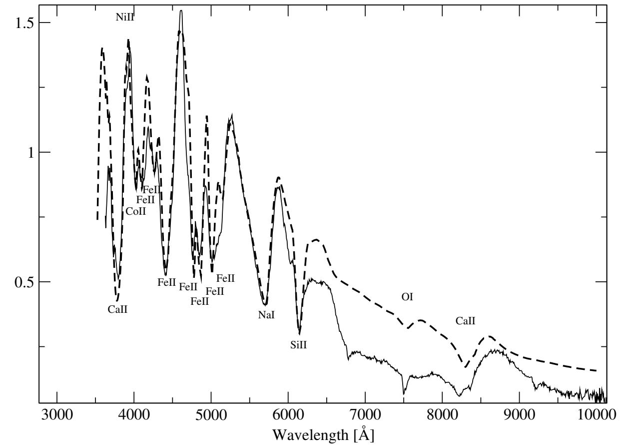

Fig. 17. Synthetic spectrum compared with SN 1999aa spectrum for day +14

Ion	τ	v_{min}	v_{max}	T_{exc}	v_e
		$10^3 \mathrm{km} s^{-1}$	$10^3 \mathrm{km} s^{-1}$	10^3K	$10^3 \mathrm{km} s^{-1}$
CaII	20	-	30	8	3
OI	0.1	-	30	5	3
SiII	1.5	10	14	8	3
FeII	5	9.5	13.5	5	2
CoII	1.6	10	20	7	3
NaI	1.2	0	30	5	5.5
NiII	3	-	10	5	5

Table 5. Synow parameters for day +14. Vphot=8500km/s, $T_{bb} = 10500$

NaI has blended with SII becoming the major component of the deep line at 5700 Å.

During the whole spectral evolution the region between 6500Å and 8000Å has become increasingly more and more difficult to match. At this epoch the discrepancy between data and synthetic spectrum are fairly evident. This is probably due to the increasing inaccuracy of the assumption of an underlying black body continuum.

6.5. +40 Days

Deeply into the iron-group core, at day +40 the supernova spectrum is mainly formed by FeII and CoII. The only

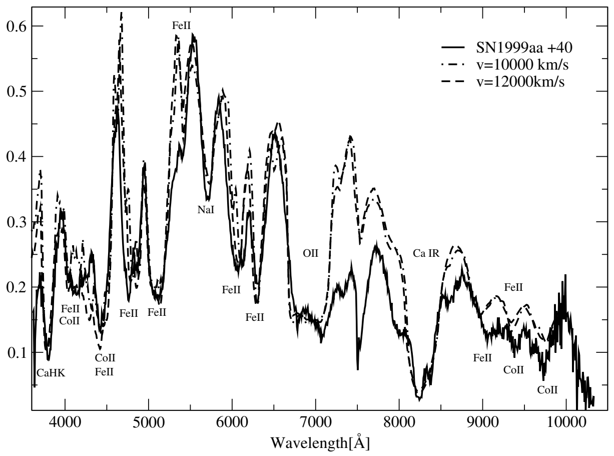

Fig. 18. Synthetic spectrum compared with SN 1999aa spectrum for day +40. Dashed line max velocity for Fe-peak core at 12000 km/s. Dotted-Dashed line max velocity for Fe-peak core at 9000 km/s

signs of IME are CaII H&K and IR. A strong and wide feature near 7000Å can be reproduced by a forbidden line of OII with a very high v_e. For the details of the composition see table 6. Some consideration has to be made about the way the components of FeII and CoII have been introduced. At this epoch the spectrum is formed into the Fe-peak core but still a part of the outer atmosphere makes a contribution. The optical depth of these elements in these two regions can in principal be different. We find useful to introduce a double layer of Fe and Co with different τ. The velocity at which this change occurs can be thought to be the iron peak core limit. Although several attempt to find the best match, it is not evident how much better an higher (12000 km/s) velocity limit fits the data with respect to a lower one (10000 km/s) (details in table 7). The two synthetic spectra are shown in fig 18.

Even if in nebular phase the SYNOW's assumption of a sharp photosphere is not expected to hold, as already found by other authors, SYNOW still can produce convincing results.

Ion	τ	v_{min}	v_{max}	T_{exc}	v_e
		10^3kms^{-1}	10^3kms^{-1}	10^3K	10^3kms^{-1}
CaII	300	-	18	8	3
OII	0.1	-	30	10	20
FeII	7	-	12	7	6
FeII	0.2	12	30	7	3
CoII	30	-	12	7	3
CoII	0.4	12	30	7	6
NaI	0.6	-	30	5	6

Table 6. Synow parameters for day +40, high velocity Fe-peak core. Vphot=7000km/s, $T_{bb} = 8000$

Ion	τ	v_{min}	v_{max}	T_{exc}	v_e
		10^3kms^{-1}	10^3kms^{-1}	10^3K	10^3kms^{-1}
CaII	300	-	17	8	3
OII	0.1	-	30	10	20
FeII	70	-	10	7	6
FeII	1.3	10	30	7	5
CoII	45	-	10	7	3
CoII	0.8	10	30	7	5
NaI	0.6	-	30	5	6

Table 7. Synow parameters for day +40, low velocity Fe-peak core. Vphot=7000km/s, $T_{bb} = 8000$

7. Discussion

7.1. Nickel and other highly ionized elements

As pointed out in (Nugent et al., 1995) the presence of highly ionized Fe and Si in the early spectra suggests higher temperature than in Branch normal SNe (see e.g. Hatano et al., 1999a, Figure 7). The innermost layers of W7 are considered to have gone through complete silicon burning, leaving only a nuclear statistical equilibrium composition such as shown in Hatano et al. (1999a, Fig. 9). The decay of the resulting ^{56}Ni to ^{56}Co and to stable ^{56}Fe would imply the presence of CoIII lines. In agreement with Hatano et al. (2002), we suggest that the NiIII lines in our pre-maximum spectra are produced by ^{54}Fe and ^{58}Ni synthesized during incomplete and complete silicon burning. If this is the case, it is not necessary to produce a model that extends the complete silicon burning in the region of intermediate mass elements or above, as originally proposed for SN 1991T-like objects. Among the current DDT models it seems that none is able to extend the presence of this ions as far out as is thought to be necessary to match the observations ($v \sim 30000$ km/s table 2). However, Höflich et al. (1998) showed that a higher initial metallicity would increase the abundance of ^{54}Fe and ^{58}Ni and this could possibly explain the observations. UV photometry and spectroscopy would yield important information to settle this issue (Lentz et al., 2000).

7.2. Carbon

The existence of an external layer of carbon has been proposed originally by Fisher et al. (1997) and re-proposed for SN 1991T by Fisher et al. (1999) based on the possible presence of the CII line on the SiII λ6355 Å region. The presence of this ion is indispensable to explain the line shape and velocity time evolution of the feature at 6150 Å for SN 1999aa, as shown in Fig. 11. We find these evidences convincing and together with the others two small lines formed by this ion even if barerly visible in the spectrum of SN1999aa we think that the identification of a detached CII layer in the outermost region of peculiar 91-T and 99aa like objects could be considered definitive. More evidences will be given anyhow in Garavini et al. (2003).

CIII λ4648.8 Å at photosphere velocities used to match the line at λ4500Å is considered probable. The presence of unburnt material deep into the IME's atmosphere region is expected in 3D models where convective flows are shown to keep refueling the inner layers with original composition. Finding unburnt material deep into the atmosphere is then theoretical possible. A first attempt to match the line on the red side of SiIII was performed by Hatano et al. (1999c) on the early spectra of SN1997br but the velocity range in which CIII would be present could not match the overall composition. They then mentioned the possibility that HeII could be responsible for the absorption but this look improbable for SNIa since this would imply a non-thermal ionization from the decay of radioactive elements. Thomas et al. (2003) tentatively suggested the possibility that the same line in SN2000cx could be matched by a high velocity Hydrogen Hβ. In our spectrum day 11 prior to maximum spectrum on SN1999aa this would not be possible because the Hα line would produce a strong absorption in the SiII λ 6150 Å region that is not found in the data.

If the identification of CII and possibly of CIII and OIII could be confirmed it would favor the presence of an unburned region of C+O rich composition, as shown in Fig. 5 in (Hatano et al., 1999a). A final word on this question can only be said using detailed radiative transfer models.

7.3. Silicon

The time evolution of the Doppler blue-shift of SiII around and after B maximum shows that this ion is confined within a thin velocity range, not only for SN 1999aa but also for SN 1997br, SN 2000cx and SN 1991T. Independent evidence for SN 1999aa is given by the SYNOW spectra were velocities between 10000 km/s and 15000 km/s where needed to match the observations when the photosphere velocity dropped below 9500 km/s; see table 3. The same holds for SN 1997br (Hatano et al., 2002) and for SN 1991T (Fisher et al., 1999). No complete SYNOW synthetic spectra are available for SN 2000cx but from the minima of the lines it seems to be formed in a slightly higher velocity layer; that velocity is stable around 12000 km/s. For a normal Type Ia supernova, such as SN 1994D, the Si rich layer extends out to 27000 km/s.

7.4. High velocity calcium

The presence of an high velocity component is strongly constrained by the presence of the blue wiggles Ca II IR triplet. The strength of the bluest of the two high velocity absorptions is almost the double compare to the red one. This cannot be reproduced by a simple 1D model but needs the study of the geometry of the atmosphere by mean of a three dimensional modeling as the one proposed for SN2001el by Kasen et al. (2003). The difference intensity of this absorptions can be reproduced by an high velocity clump of material viewed from a line of sight that makes it barely covered the photosphere. In our synthetic spectra the evidences for the external component of CaII come also from the Ca II H&K. To reproduced completely the broad profile of this line at day -11 and the blue minimum around maximum the high velocity component is needed. When the temperature of the atmosphere drops down, and the photosphere recedes into the inner layers, low ionization Fe-peak group lines become more important in the Ca H&K region, in this case reproducing accurately the line profile becomes difficult. However we could not match the Ca H&K absorption showed at day -11 as well as the one at day -1 by other means.

8. Conclusions

We have presented detailed analysis of the spectrum development of SN 1999aa. The overall evolution of spectral features suggests a peculiar object with a hot exterior and possible signs of high metallicity. The line identification for the earliest spectrum, if confirmed, would suggest an unburnt region and highly ionized ions consistent with C+O rich composition. The tentative identification of CIII $\lambda 4648.8$ Å at photosphere velocity, would shows the presence of original material in the IME's region of the atmosphere. The spectral evolution of SN 1999aa shows that IME's populate a narrow velocity window. Similar evidences are found in other well known peculiar supernovae explosions (e.g. SN 1991T, SN 1997br and SN 2000cx). The comparison with other peculiar objects of the same kind suggests that the transition between IME to iron-peak dominant composition can occur at slightly different phase. The real origin of the differences between normal supernovae and peculiars probably depends on several factors. The increasing of the temperature has been shown to be able to account for some of the peculiarities (Nugent et al., 1995). Iwamoto et al. (1999) presented a model (CS15DD3) with ^{58}Ni and ^{54}Fe extending to higher velocities and with the presence in the same region of intermediate mass elements. As already proposed for SN 1997br by Hatano et al. (2002) this is consistent with the observed and synthetic spectra presented here for SN 1999aa, but does not fully explain the peculiarities of this objects.

New accurate optical and infrared spectra as well as spectropolarimetry studies are needed to support the evolving degree of complexity of the models proposed and to give a complete explanation of the physics of supernovae explosions. SN 1999aa provides clear evidence, however, that perhaps a single model could explain both normals and peculiar SN 1991T-like SNe and that this object might be positioned between the two extremes on a single class of events.

References

Aldering, G. 2000, "Type Ia Supernovae & Cosmic Acceleration," *AIP Conference Proceeding: Cosmic Explosions*, ed. S. S. Holt & W. W. Zhang, Woodbury, New York: American Institute of Physics.

Arbour, R. 1999, IAU Circ. 7108

Branch, D.; Lacy, C. H.; McCall, M. L.; Sutherland, P. G.; Uomoto, A.; Wheeler, J. C.; Wills, B. J., 1983, ApJ, 270, 123B.

Branch D., Fisher A., Nugent P., 1993, AJ 106, 2383.

Branch D. 2000 astro-ph/0012300

Branch D, Baron E. Jeffery J. D. astro-ph/0111573

Branch D, 2001 PASP,113,169B

Cardelli J. A., Clayton G. C., Mathis J. S., 1989, ApJ, 345, 245.

Filippenko Alexey V. 1992 ApJ, 384, L15.

Filippenko Alexey V. 1997 ARA&A, 35, 309F.

Filippenko, A. V., Li, W. D., Leonard, D. C. 1999, IAU Circ. 7108

Fisher A., Branch D., Hatano K., Baron E., 1999, MNRAS, 304, 67-74.

Fisher A., Branch D., Nugent P., Baron E., 1997, ApJ, 304, L89

Folatelli et al. 2003, in prep.

Folatelli et al. 2003, in prep.

Gamezo Vadim N., Khokhlov Alexei M., Oran Elaine S., Chtchelkanova Almadena Y., Rosenberg Robert O. 2003 Sci, 299, 77G.

astro-ph0105490

Gómez G.; López R., 1998 AJ, 115, 1096G.

Goobar A., Perlmutter S., 1995, ApJ, 450, 14.

Hatano K., Branch D., Fisher A., Millard J., Baron E., 1999, ApJ, 121, 233.

Hatano K et al., 1999, ApJ, 525, 881-885.

Hatano, Kazuhito; Branch, David; Qiu, Y. L.; Baron, E.; Thielemann, F.-K.; Fisher, Adam 2002 NewA,7,441H

Hatano K.,Branch D.,Lentz E.J.,Baron E.,Filippenko A. V., 2000, ApJ, 543, L49.

Hatano K., Branch D., Qiu Y.L., Baron E., Thielemann F.-K., 2002, NewA, 7, 441.

Hillebrandt et al ARAA 2000, 38, 191.

Hoyle F., Fowler W.A., 1960 AJ, 132, 565.

Horne, K. 1986, PASP, 98, 609

Höflich P., 1995, ApJ, 443, 89-108.

Höflich P., Wheeler J. C.,Thielamann F.-K., 1998, ApJ, 495, 617.

Iwamoto K., Brachwitz F., Nomoto K., Kishimoto N., Umeda H., Raphael Hix W., Thielemann F-K., 1999, ApJS, 125

Jeffrey D. J., Leibundgut , Kirshner R. P., Benetti S., Branch D. & Sonnenborn G., 1992, ApJ, 397, 304.

Kasen D., Nugent P., Wang L., Howell D.A., Wheeler H. J. G., Hoeflich P., Baade D., Baron E., Hauschildt, P.H., astro-ph, 0301312.

Khokhlov A.M., 1991, A&A, 245, 114.

Kirshner R. P. et al 1993 ApJ, 415, 589.

Krisciunas K., Hastings N.G., Loomis K., McMillan R., Rest A., Riess A. G., Stubbs C., 2000 ApJ, 539, 658.

Leibundgut et al AAR 2000, 10, 179.

Leibundgut 1991ApJ, 371 L23

Lentz E.J., Baron E., Branch D., Hauschildt P.H.,Nugent P., 2000, ApJ, 530, 966-976.

Lentz E.J., Baron E., Branch D., Hauschildt P.H. 2001 ApJ, 547, 402L.

Lentz E.J., Baron E., Branch D., Hauschildt P.H., 2001, ApJ, 557, 266-278.

Lentz E.J., Baron E., Branch D., Hauschildt P.H., 2001, ApJ, 547, 402.

Li W.D. et al. 1999 ApJ 117, 2709-2724.

Li W.D. et al. 2001a, PASP, 113, 1178-1204.

Li W. et al. 2001b, ApJ, 546, 734.

Marquardt Donald W.,J. Soc. Indust. Appl. Math. Vol. 11. No. 2, June 1963

Mazzali P.A, Danzinger I.J., Turatto M.. 1995 A&A, 297, 509-534.

Mazzali Paolo A. 2001 MNRAS, 321, 341-346.

Nakano, S., Kushida, R. 1999, IAU Circ. 7109

Nomoto K., Thielemann F.-K., Yokoi K. 1984, ApJ, 286, 644.

Nugent, P., Aldering, G., & The Nearby Campaign 2000, Supernovae and gamma-ray bursts: The Greatest Explosions Since the Big Bang: poster papers from the Space Telescope Science Institute Symposium, May 1999 / Mario Livio, Nino Panagia, Kailash Sahu, editors. [Baltimore, Md.] : Space Telescope Science Institute, [2000]., p.47, 47.

Nugent P.,Baron E., Branch D., Fisher A., Hauschildt P.H, ApJ 485, 812-819.

Nugent P., Phillips M., Baron E., Branch D., Hauschildt P.H, ApJ 455, 147.

Patat, F.; Benetti, S.; Cappellaro, E.; Danziger, I. J.; della Valle, M.; Mazzali, P. A.; Turatto, M. 1996, MNRAS, 278, 111-124.

Perlmutter et al. 1999, ApJ, 517, 565

Phillips, M. M.; Lira, Paulina; Suntzeff, Nicholas B.; Schommer, R. A.; Hamuy, Mario; Maza, Jos. 1999, AJ, 118, 1766

Phillips, M. M.; Wells, Lisa A.; Suntzeff, Nicholas B.; Hamuy, Mario; Leibundgut, Bruno; Kirshner, Robert P.; Foltz, Craig B. 1992 AJ,103, 1632P

Qiao, Q. Y., Wei, J. Y., Qiu, Y. L., Hu, J. Y. 1999, IAU Circ. 7109

Riess et al. 1998, AJ, 116, 1009

Ruiz-Lapuente P., Cappellaro E., Turatto M., Gouiffes C., Danziger I. J., della Valle M., Lucy L. B., 1992ApJ, 387L, 33R.

Schlegel, D. J., Finkbeiner, D. P., Davis, M. 1998, ApJ, 500, 525

Thomas R. C., Branch D., Baron E., Nomoto K., Li W., Filippenko A. V., 2003, astro-ph/0302260

Wheeler J. C.; Harkness R. P. 1990 Rep. Prog. Phys., 53, 1467-1557

Woosley S. E., Weaver T. A., 1986 ARA&A 24, 205.

Yamaoka H., Nomoto K., Shigeyama T., Thielamann F.-K., 1992, Apj, 393,55.